Chain Structures of Surface Hydroxyl Groups Formed via Line Oxygen Vacancies on TiO_2(110) Surfaces Studied Using Noncontact Atomic Force Microscopy

Yoshimichi Namai* and Osamu Matsuoka

Polymerization Catalysis Group, Catalysis Science Laboratory, Mitsui Chemicals, Inc., 580-32 Nagaura, Sodegaura, Chiba 299-0265, Japan

Received: July 18, 2005

Structures of surface hydroxyl groups arranged on a reduced TiO_2(110) surface that had line oxygen vacancies were studied using noncontact atomic force microscopy (NC-AFM). NC-AFM results revealed that by increasing the density of oxygen vacancies on the TiO_2(110) surface, line oxygen vacancies were formed by removal of oxygen atoms in a bridge oxygen row on the TiO_2(110) surface. After the TiO_2(110) surface with the line oxygen vacancies was exposed to water, the surface showed hydroxyl chain structures that were composed of hydroxyl groups linearly arranged in a form of two rows on the line oxygen vacancies and on a neighboring bridge oxygen row. In-situ NC-AFM measurements of these surfaces exposed to water at room temperature revealed that hydroxyl chain structures were formed at the line oxygen vacancy. Annealing above 500 K was sufficient to remove the hydroxyl chain structures on the TiO_2(110) surface and allowed line oxygen vacancies to reappear on the surface. The line oxygen vacancies are active sites for water dissociation. In conclusion, the formation of the hydroxyl chain structure suggests that the surface hydroxyl groups on a TiO_2(110) surface can be controlled by preparing oxygen vacancy structures on the surface.

1. Introduction

Surface hydroxyl groups are important in the modification of the reactivity of oxide surfaces. Artificial control of surface hydroxyl groups is crucial because some hydrogen atoms bound to surface oxygen atoms are positively charged and thus change the surface acidity of oxides.[1] On an oxide surface, exposed coordinatively unsaturated metal cations and oxygen anions, which are Lewis acid and Brϕnsted base sites, respectively, change to Brϕnsted acid sites according to adsorption of surface hydroxyl groups. Hydrogen adatoms therefore play a critical role in the surface properties and reactivity of oxide surfaces.[2] To improve the reactivity of oxide surfaces, the structure of surface hydroxyl groups on oxide surfaces in catalytic reactions must therefore be controlled. In this current study, to try controlling the arrangement of hydroxyl groups on oxide surfaces, a well-defined titanium dioxide (TiO_2)(110) surface was used as a model surface.

TiO_2 has numerous applications, such as heterogeneous catalysis, solar cells, gas sensors, corrosion-protective coatings, optical coatings, and gate insulators for the new generation of MOFSET, etc.[2,3] The rutile-type TiO_2(110) surface, which is the most stable crystal face, has been extensively studied as a model surface to understand the structure and dynamics of adsorption molecules.[3] Surface hydroxyl groups on TiO_2(110) surface can be introduced by exposure to atomic hydrogen[4] and water.[5] Despite the weak interaction between molecular hydrogen and TiO_2, atomic hydrogen adheres to TiO_2(110) surfaces at room temperature (RT).[6] Water molecules dissociate at surface oxygen vacancy sites[3,5,7−16] and step sites,[9,17] and can lead to two bridging hydroxyl groups per oxygen vacancy site (i.e., hydroxylation). Therefore, if oxygen vacancy structures on TiO_2(110) surfaces can be controlled, then the arrangement of hydroxyl groups on such surfaces should be easily controlled by exposure to water at RT. Atomic-scale structures of TiO_2-(110) surfaces and surface features such as point oxygen vacancy and hydroxyl groups and Ti_2O_3 added row structures on the TiO_2(110) have been studied by scanning tunneling microscopy (STM) and noncontact atomic force microscopy (NC-AFM).[3] However, various oxygen vacancy structures and their reactivity of TiO_2(110) surfaces in atomic-scale have not been studied yet.

NC-AFM is an effective tool for observing surface structures at the atomic-scale, dynamic behavior of atoms and molecules and surface reaction mechanisms on various surfaces such as semiconductors, ionic crystals, and metal oxides.[18] NC-AFM can effectively visualize oxygen vacancies[19] and hydroxyl groups[20] on TiO_2(110) surfaces, because the image contrast of an oxygen vacancy and a hydroxyl group differs. Recent STM studies show that oxygen vacancies and hydroxyl groups on a TiO_2(110) surface can be distinguished.[12,13] In this case, however, the oxygen vacancy and the hydroxyl group are visualized at the same contrast. Therefore, NC-AFM is an effective tool to distinguish oxygen vacancies and hydroxyl groups on bridge oxygen rows of the TiO_2(110) surface.

In this study, we observed line oxygen vacancies on a reduced TiO_2(110) surface for the first time and elucidated that hydroxyl groups arranged on TiO_2(110) surfaces reflecting the structure of line oxygen vacancies formed on the TiO_2(110) surface by exposure to water at RT. The arranged structure was then visualized using NC-AFM. NC-AFM measurements revealed that the line oxygen vacancy consisted of removal of oxygen atoms on the bridge oxygen row of the TiO_2(110) surface accompanying the increasing of the density of oxygen vacancies on the surface. Also, successive NC-AFM observations of a same area on the TiO_2(110) surface before and after exposure to water revealed that hydroxyl chain structures were formed

* Corresponding author. Tel: +81-438-64-2321, Fax: +81-438-64-2374, E-mail: Yoshimichi.Namai@mitsui-chem.co.jp.

10.1021/jp058210r CCC: $30.25
Published on Web 11/30/2005

at the line oxygen vacancy due to the linear arrangement of hydroxyl groups.

2. Experimental Section

The NC-AFM used for the observations was an ultrahigh vacuum (UHV) AFM (JAFM-4610; JEOL) equipped with ion gun optics (JEOL) with a base pressure of 1.5×10^{-10} Torr. NC-AFM cantilevers were conductive silicon cantilevers with a typical resonant frequency of 315 kHz and spring constant of 48 N m^{-1} (MikroMasch). Because the cantilever tips were not treated by Ar^+ ion sputtering, they were probably initially covered with a native oxide.

First, the TiO_2(110) surface was visualized by using the topographic mode of the NC-AFM. During the scanning of the TiO_2(110) surface, (a) the resonant frequency shift (Δf) of the cantilever was regulated by using the FM detection method[21] and was kept constant by applying a voltage to the *z*-direction of the piezo scanner, (b) a bias voltage (V_s) between +1 V and +1.5 V was applied to the sample to compensate the average contact potential between the tip and the sample surface,[22,23] (c) the oscillation amplitude (ΔA) of the cantilevers was approximately 15 nm, and (d) the measurements were done at RT. Then, TiO_2(110) samples that were $6.5 \times 1 \times 0.25$ mm^3 (Furuuchi Chemicals) were cleaned by repeated cycles of Ar^+ ion sputtering (2.5 mA at 3 keV for 180 s) and UHV annealing (at 950 K for 180 s). Finally, the surfaces were exposed to water (Aldrich), which had been purified by repeated freeze−pump−thaw cycles, by introducing the water into the NC-AFM chamber via a gas doser.

3. Results

3.1. NC-AFM Observations of a Line Oxygen Vacancy on a TiO_2(110) Surface. First, structures of line oxygen vacancies on a reduced TiO_2(110) surface were examined using NC-AFM. Figure 1a shows a NC-AFM image of line oxygen vacancies (dark rows on the bright rows in Figure 1a) formed by removal of more than two oxygen atoms on the bridge oxygen rows of the reduced TiO_2(110) surface. Figure 1b shows a model of the line oxygen vacancy based on the bulk-terminated model of TiO_2(110)−(1 × 1) surface. The bridge oxygen rows protruding over the surface correspond to bright rows, and the point oxygen vacancies correspond to dark spots.[19] The oxygen vacancy density of a TiO_2(110) surface with line oxygen vacancies on the surface was estimated at $(2.0-2.4) \times 10^{13}$ cm^{-2}, whereas the oxygen vacancy density of a TiO_2(110) surface, which was mostly point oxygen vacancies, was $(0.7-1.2) \times 10^{13}$ cm^{-2}. This is consistent with previously reported values of $(0.5-1.6) \times 10^{13}$ cm^{-2} obtained by NC-AFM observation of TiO_2(110) surfaces annealed at 900 K for 180 s.[19] In this range of oxygen vacancy density,[19] most oxygen vacancies on the surface are point oxygen vacancies. Our results are consistent with this observation. To clarify the structure of line oxygen vacancies, NC-AFM measurements of a TiO_2(110) surface with numerous oxygen vacancies by longer annealing of the surface were performed. Figure 2 shows the distribution of the length of line oxygen vacancies at each annealing time of 180, 300, and 600 s (at 950 K). The shortest line oxygen vacancy is consisting of two oxygen vacancies. Based on the bulk-terminated model of a TiO_2(110)−(1 × 1) surface (Figure 1b), the estimated length of the line oxygen vacancies with the removal of two oxygen atoms is about 0.6 nm. In Figure 2c, line oxygen vacancies of more than 12 nm, which were not observed in Figure 2a and 2b, slightly appeared, and line oxygen vacancies of less than 4 nm were not observed. Figure 2

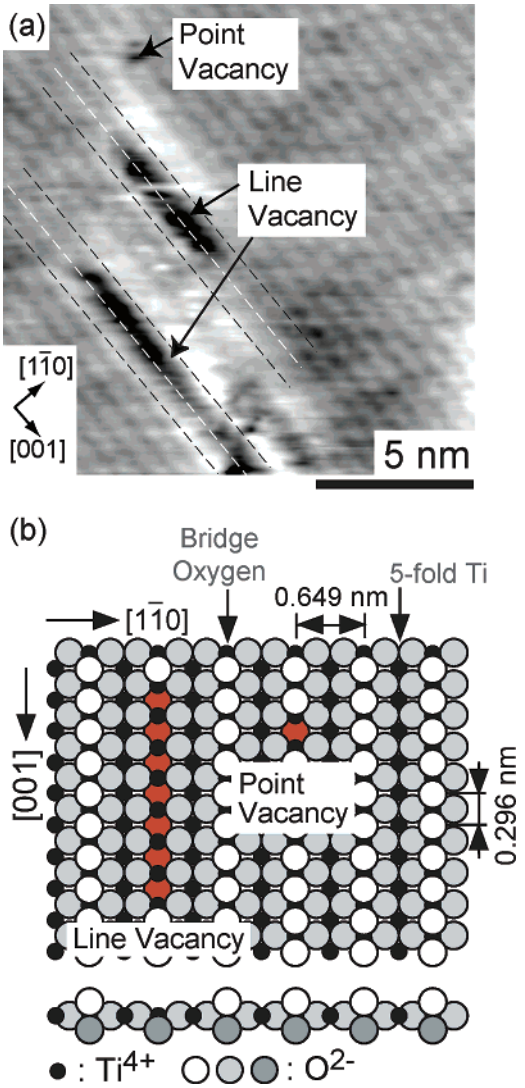

Figure 1. (a) NC-AFM image (14.7×14.7 nm^2) of a reduced TiO_2-(110) surface with line oxygen vacancies. $\Delta f \sim 63$ Hz. White and black lines represent bridge oxygen rows of the TiO_2(110) surface. (b) Structural model of the line oxygen vacancy and the point oxygen vacancy on the TiO_2(110)−(1 × 1) surface.

indicated that the length of the line oxygen vacancy on TiO_2-(110) surfaces increased with increasing annealing time. Therefore, we consider that Figure 2 reveals formation of line oxygen vacancy by increasing of the annealing time. The estimated oxygen vacancy density on the surface annealed for 300 s (Figure 2b) was $(3.0-4.2) \times 10^{13}$ cm^{-2}, whereas that annealed for 600 s (Figure 2c) was $(5.1-5.9) \times 10^{13}$ cm^{-2}. Oxygen point vacancies were seldom observed when the surface was annealed longer than 600 s. Therefore, the length of the line oxygen vacancy and the density of the oxygen vacancy on TiO_2(110) surfaces increased with increasing annealing time. In summary, the NC-AFM observations clearly reveal that formation of line oxygen vacancy depended on the oxygen vacancy density. STM measurement of the TiO_2(110) surface annealed at 950 K for 300 s revealed a bright line on a dark row, corresponding to a bridge oxygen row on the surface. Therefore, line oxygen vacancies on the reduced TiO_2(110) surface were observed by both NC-AFM and STM measurements.

Figure 1a reveals that both sides of oxygen atoms surrounding the line oxygen vacancy were observed with brighter contrast. Based on the TiO_2(110)−(1 × 1) surface model shown in Figure 1b, both sides of the bridge oxygen rows adjacent to the line

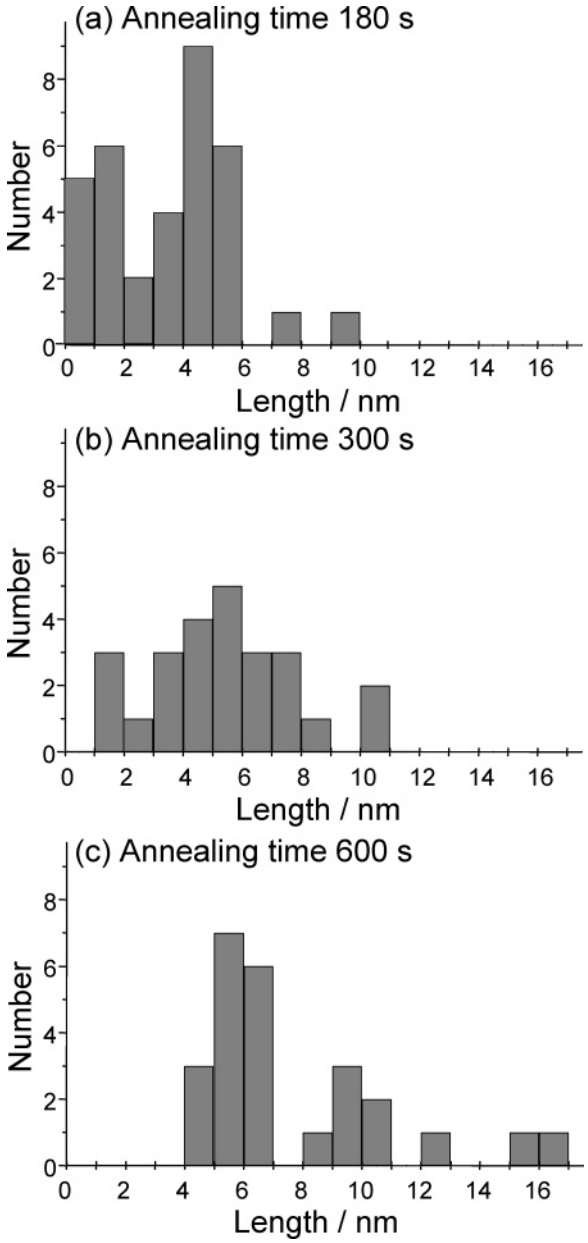

Figure 2. Distribution of the length of line oxygen vacancies on a reduced $TiO_2(110)$ surface annealed at 950 K for (a) 180 s, (b) 300 s, and (c) 600 s. The shortest line oxygen vacancy was the two oxygen vacancy, and the minimum length estimated from the bulk-terminated model of a $TiO_2(110)-(1 \times 1)$ surface was about 0.6 nm.

oxygen vacancy are equivalent sites. As revealed by the brighter contrast, these oxygen atoms surrounding the line oxygen vacancy were 0.04−0.06 nm higher in topography than oxygen atoms except for line oxygen vacancies. Here, brighter contrast surrounding the line oxygen vacancies is not an artifact such as delayed feedback during measurements, because a point oxygen vacancy was observed without enhanced contrast in NC-AFM measurements (Figure 1a).

3.2 In-situ NC-AFM Observations of Hydroxyl Chains Formed on the $TiO_2(110)$ Surface with the Line Oxygen Vacancy. Next, the reactivity of line oxygen vacancies on the $TiO_2(110)$ surface against water molecules was examined. After exposing the $TiO_2(110)$ surface with the line oxygen vacancy to water (7.5×10^{-7} Torr for 120 s), line protrusions appeared in a form of two rows on bridge oxygen rows of the surface (Figures 3a and 3b). Based on the bridge oxygen rows, the estimated height of this line protrusion was 0.03−0.05 nm. Figure 3c shows the adsorption model of this line protrusion based on the bulk-terminated model of a $TiO_2(110)-(1 \times 1)$ surface. Line protrusions were not observed on the $TiO_2(110)$ surface before exposure to water. Based on NC-AFM observations of the surface after exposure to water, the line protrusions did not change during scanning the surface. The length of the line protrusions (Figures 3a and 3b) corresponds to the length of line oxygen vacancies on the $TiO_2(110)$ surface observed using NC-AFM before water exposure. Although three different TiO_x added-row models for the $TiO_2(110)-(1 \times 2)$ structure have been proposed (Ti_2O_3 added-row model,[27−30] Ti_3O_5 added-row model,[31] and Ti_3O_6 added-row model[32,33]), none of these models could be applied here because the observed line protrusion was actually two adjoining rows with bright contrast on bridge oxygen rows of the $TiO_2(110)$ surface.

Because molecular water does not adsorb on $TiO_2(110)$ surfaces at RT,[5] these line protrusions might be structures that consist of hydroxyl groups and are formed by dissociative adsorption of water molecules at oxygen vacancy sites. Dissociative adsorption of water occurring on oxygen vacancy sites of $TiO_2(110)$ surfaces was previously confirmed by STM and other experimental results such as high-resolution electron energy loss spectroscopy (HREELS), temperature programmed desorption (TPD), X-ray photoemission spectroscopy (XPS).[8−16] Based on these results and our results, formation of the line protrusion suggests dissociative adsorption of water molecules at the line oxygen vacancy. Here we call this line protrusion "hydroxyl chain" structure.

The dynamic process to form hydroxyl chain structures on the $TiO_2(110)$ surface with line oxygen vacancies by exposure to water at RT was observed by in-situ NC-AFM measurements. Figures 4a and 4b show NC-AFM images of the same area of the $TiO_2(110)$ surface with the line oxygen vacancy before and after exposure to water at 7.5×10^{-10} Torr at RT for 91 s. Exposure to water apparently filled in the line oxygen vacancy on the $TiO_2(110)$ surface (Figure 4b) and caused a line protrusion to appear at the line oxygen vacancy and at the bridge oxygen rows adjacent to the line oxygen vacancy. The height of this line protrusion was 0.02−0.04 nm, which is consistent with the height of the line protrusion on the $TiO_2(110)$ surface measured in Figure 3b, indicating that this line protrusion is a hydroxyl chain structure appearing in a form of two rows on the surface. Therefore, in-situ NC-AFM observations revealed that the hydroxyl chain structure was formed at the line oxygen vacancy. Because annealing above 500 K, which enables dissociative recombination of hydroxyl groups,[8−11,15,16] was sufficient to remove the hydroxyl structures on the $TiO_2(110)$ surface, line oxygen vacancies reappeared on the surface. In summary, NC-AFM measurements revealed that line oxygen vacancies are key in the formation of hydroxyl chain structures.

4. Discussion

4.1 Line Oxygen Vacancies on a $TiO_2(110)$ Surface. Using STM, Fischer et al.[34−36] studied defect structures such as point defects and line defects on $TiO_2(110)$ surfaces and proposed a geometric model of [001] line defects that are produced by removal of oxygen and titanium atoms from [001] rows. However, they adopted a different interpretation of the bright rows in STM, namely, the rows are caused by bridging oxygen rows.[3] Also, their line defect resembled line defect structures that consisted of added rows with an overall Ti_2O_3 composition running along the [001] direction and that eventually cover the entire surface in a (1×2)-type overlayer.[37] Therefore, their line defects might correspond to additional TiO_x species, which

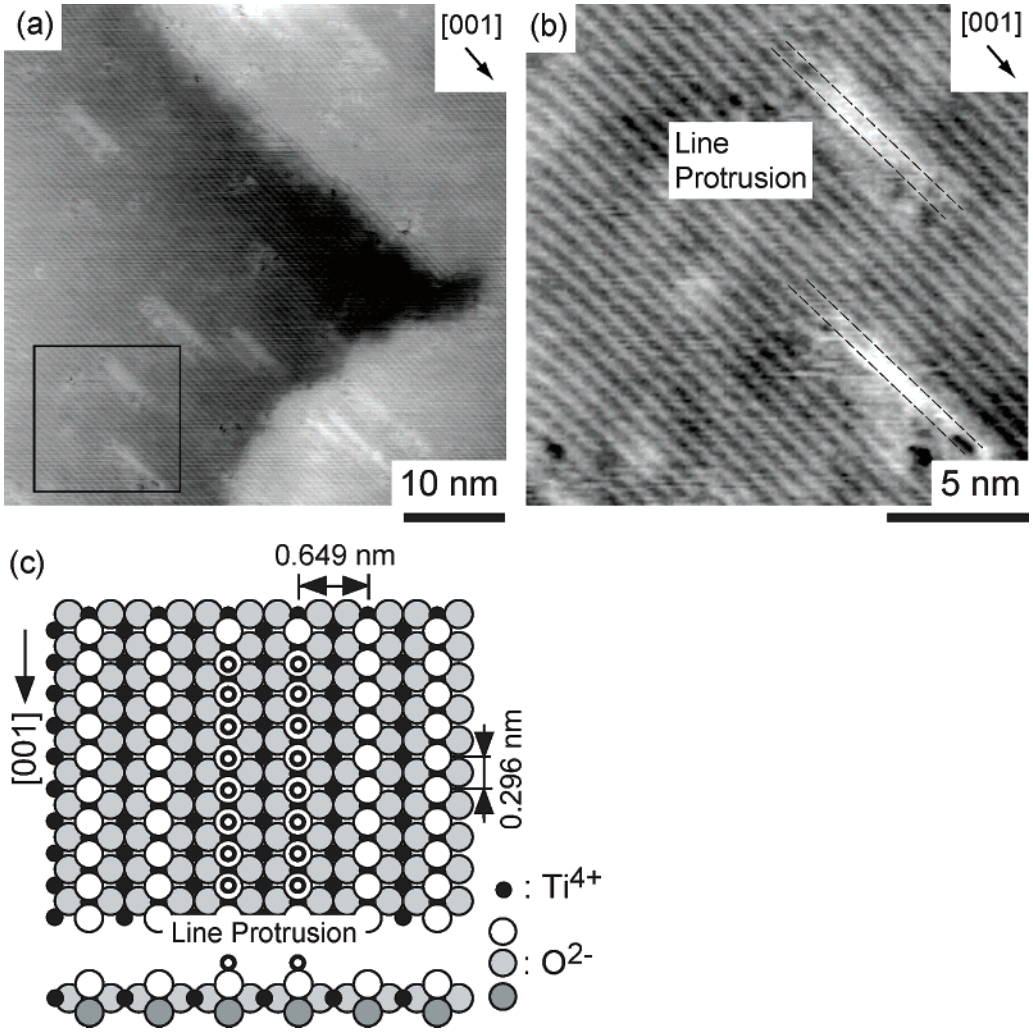

Figure 3. (a) NC-AFM image (49.2 × 49.2 nm^2) of a reduced TiO_2(110) surface after exposure to water at room temperature (7.5×10^{-7} Torr for 120 s). $\Delta f \sim 93$ Hz. Black lines represent bridge oxygen rows of the TiO_2(110) surface. (b) Enlarged NC-AFM image of the rectangular area (17.4 × 17.4 nm^2) in (a). (c) Structural model of the line protrusion on the TiO_2(110)−(1 × 1) surface.

are formed by reaction between gaseous oxygen and interstitial titanium ions with high diffusivity at elevated temperatures.[29,32,33]

Line oxygen vacancies revealed by our NC-AFM observations (Figure 1a) could be identified as oxygen vacancy structures appearing due to removal of many surface oxygen atoms. Line oxygen vacancies should appear as dark rows because bright rows correspond to bridge oxygen rows protruding above the surface.[19] In our results, dark rows on bright oxygen rows were observed using NC-AFM (Figure 1a), and therefore these dark rows can be identified as line oxygen vacancies on the TiO_2-(110) surface.

We also observed Ti_2O_3 added-row strands on TiO_2(110) surfaces using NC-AFM (results not shown). These appeared as bright strands in the center of two bridge oxygen rows, and based on the bridge oxygen rows. Based on NC-AFM observation (Figure 1a), these species clearly differ from line oxygen vacancies, which appear as dark rows on bright oxygen rows. STM observations also confirmed the Ti_2O_3 added rows and line oxygen vacancies on the TiO_2(110) surface. The difference in the formation mechanism of line oxygen vacancies and Ti_2O_3 added-rows, however, remains unclear.

Considering the structures of the line oxygen vacancies observed in Figure 1a, the line oxygen vacancy corresponds to a missing row model for the (1 × 2) structure. First-principles total-energy calculations using density functional theory (DFT) previously showed that the added-row Ti_2O_3 model[27] has a lower surface energy than dose the missing row model,[38] and that a (1 × 2) structure with a missing row has similar surface energy to a (2 × 1) structure with only a point oxygen vacancy.[39] The missing-row model, therefore, cannot explain the (1 × 2) structure revealed by STM. Our NC-AFM measurements, however, revealed that line oxygen vacancies appeared on bridge oxygen rows of a reduced TiO_2(110) surface (Figure 1a). Although TiO_2(110) surfaces have been extensively studied by using STM and NC-AFM,[3] line oxygen vacancies have not yet been reported. Further study is needed to clarify the formation mechanism of the line oxygen vacancy.

Line oxygen vacancies were not observed on the TiO_2(110) surface until the density of oxygen vacancies reached 2.0×10^{13} cm^{-2} in our NC-AFM experiments (see section 3.1). This indicates that line oxygen vacancies can be therefore formed by increasing the density of oxygen vacancies on TiO_2(110) surface. Previous NC-AFM studies of CeO_2(111) surfaces revealed that multiple vacancies such as line oxygen vacancies were observed on the surfaces until the density of oxygen vacancies reached 1.0×10^{13} cm^{-2}.[24−26] Based on those studies, if the density of oxygen vacancies is quite low ($<1.0 \times 10^{13}$ cm^{-2}), the CeO_2(111) surface might reach equilibrium, in which the entropy factor might overcome the energy factor during annealing of the surface, thus allowing the point oxygen vacancies to become the dominant species on the surface.[24−26]

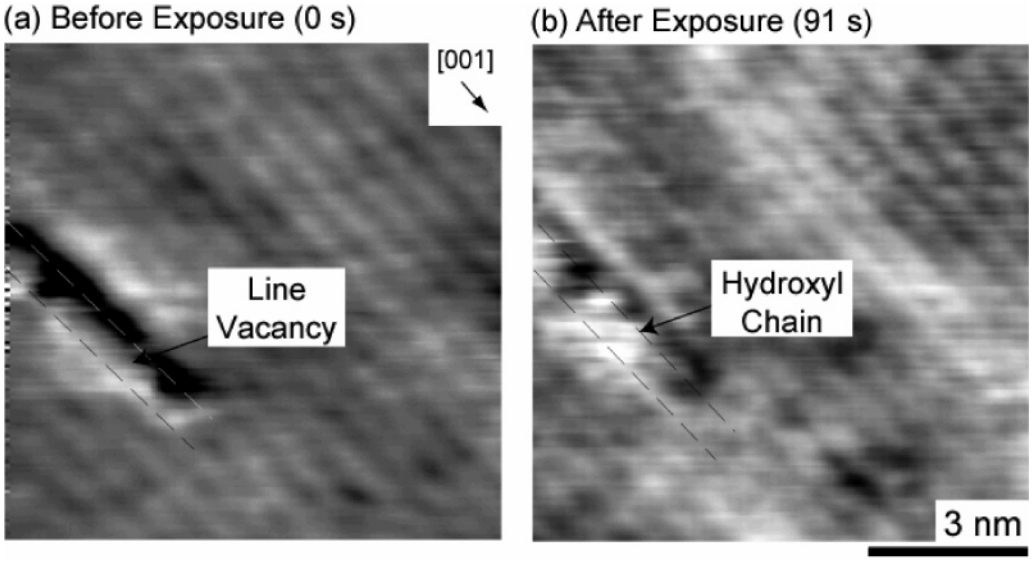

Figure 4. (a, b) NC-AFM images (9.2×9.2 nm^2) of the same area of a reduced TiO_2(110) surface with the line oxygen vacancy before and after the surface was exposed to water at RT (7.5×10^{-10} Torr). $\Delta f \sim 62$ Hz. Original scan area was 27.5×27.5 nm^2. The line oxygen vacancy was filled by dissociative adsorption of water within 91 s, and hydroxyl chain structure appeared on two bridge oxygen rows. White and black lines represent bridge oxygen rows of the TiO_2(110) surface.

Most of the oxygen vacancies on a TiO_2(110) surface therefore might be point oxygen vacancies because the TiO_2(110) surface reaches equilibrium when the density of oxygen vacancies is low ($<1.2 \times 10^{13}$ cm^{-2}).

Figures 1a and 4a show that both sides of bridge oxygen rows surrounding a line oxygen vacancy appeared with brighter contrast than other bridge oxygen rows. The brighter contrast in these NC-AFM images resulted from the topography or a distribution of charge density, which led to a different contrast due to differences in the interaction between the tip and the sample.[18] Differences in charge density due to removal of oxygen atoms on oxide surfaces might affect the image contrast. In general, considering the bulk-terminated model of TiO_2-(110)$-(1 \times 1)$ (Figure 1b), point oxygen vacancies on the TiO_2-(110) surface reduced the two 6-fold coordinated Ti^{4+} ions to two 5-fold coordinated Ti^{3+} ions on a bridge oxygen row. However, 5-fold coordinated Ti^{4+} rows and bridge oxygen rows adjacent to the line oxygen vacancies do not probably affect the differences in the charge density, because the 5-fold coordinated Ti^{3+} ions on line oxygen vacancy arrange along the [001] direction. If the charge density of the titanium ions contributed to the image contrast, then the contrast of the line oxygen vacancy itself should change. However, such a tendency was not observed in our NC-AFM measurements. The brighter contrast therefore depends not on the distribution of the charge density but on a geometric effect. Recent NC-AFM observations of CeO_2(111) surfaces revealed that line oxygen vacancies are stabilized by a local reconstruction, where edge oxygen atoms surrounding the multiple oxygen vacancies are displaced, thus producing enhanced brightness due to a geometric effect.[24−26] Although the resolution of NC-AFM images obtained here made it difficult to confirm the displacement of bridge oxygen rows surrounding the line oxygen vacancy, we consider that the enhanced contrast is due to structural changes of the surroundings of the line oxygen vacancy.

Lindan et al.[39] performed plane-wave pseudopotential DFT calculations of electronic and physical structures on reduced TiO_2(110) surfaces with (2×1) and (1×2) surface reconstructions. They found that, in the unit cell of the (2×1) structure, in-plane oxygen atoms surrounding point oxygen vacancies on a bridge oxygen row do not change in the [1−10] direction.[39] In the unit cell of the (1×2) structure, although in-plane oxygen atoms, which are both sides of 5-fold coordinated Ti^{4+} rows, surrounding two oxygen vacancies on a bridge oxygen row are displaced 0.036 nm in the [110] direction from the position in a TiO_2(110)$-(1 \times 1)$ bulk-terminated model due to a distortion of 0.01 nm toward the oxygen vacancies in the [1−10] direction, the neighboring bridge oxygen rows remain the position in the bulk-terminated model.[39] In the line oxygen vacancy formed by removal of oxygen atoms, however, the bridge oxygen rows surrounding the line oxygen vacancy might be slightly displaced from the bulk-terminated positions by the local reconstructions, which were formed to stabilize the line oxygen vacancy. In conclusion, the enhanced contrast of bridge oxygen rows surrounding the line oxygen vacancies might be due to slight structural changes in the bridge oxygen rows.

4.2 Hydroxyl Chain Structures on a TiO_2(110) Surface with Line Oxygen Vacancies. In oxide surfaces, water dissociative adsorption occurs at cation sites, which act as Lewis acid sites and can interact with molecules, and at anion sites, which act as Brønsted basic sites and can extract hydrogen ions from adsorbates. On each TiO_2 surface, water molecules are expected to bind at 5-fold coordinated Ti^{4+} ions with O−H bonds pointing away from the surface.[3,5] Henderson[9] studied the difference in dissociative adsorption of water on the (100) and (110) surfaces of rutile-type TiO_2 using TPD. On a nearly stoichiometric TiO_2(110) surface, which is a nearly oxygen-vacancy-free surface, water dissociation appears to be inactive, because the bridging oxygen sites on the TiO_2(110) surface are too distant from the binding sites of water to form hydrogen-bonding interactions with water that might facilitate O−H bond dissociation (0.325 nm distance between the oxygen atom of the water molecule adsorbed on 5-fold coordinated Ti^{4+} site and the nearest anion site, namely, 2-fold coordinated bridging O^{2-} site).[9] In contrast, on a TiO_2(100) surface, water dissociation appears to be active, because the distance between the oxygen atom of an adsorbed water molecule and a 2-fold coordinated bridging O^{2-} site is about 0.28 nm.[9] This distance is sufficient to yield a weak hydrogen-bonding interaction. In a defective TiO_2(110) surface with point oxygen vacancies on bridge oxygen rows of the TiO_2(110) surface, the distance between the oxygen atom of a water molecule adsorbed on the point

oxygen vacancy and the next oxygen atom is 0.296 nm.[9] This distance is also sufficient to yield a weak hydrogen-bonding interaction.

In the line oxygen vacancies on a TiO_2(110) surface, if a line oxygen vacancy does not form a reconstructed structure, the distance between the nearest anion site (bridge oxygen row adjacent to the line oxygen vacancy) and the oxygen atom of a water molecule on 5-fold Ti^{4+} site and line oxygen vacancy site is 0.325 and 0.649 nm (estimated from Figure 1b), respectively, except at both ends of the line oxygen vacancy, where the distance between the oxygen atom of a water molecule adsorbed on the vacancy of both ends of the line oxygen vacancy and the next oxygen atom is 0.296 nm.[9] The nonreconstructed line oxygen vacancy is therefore an inactive site for water dissociation because a water molecule adsorbed on the line vacancy cannot interact with the anion site. Hydroxyl chains were observed, however, on the line oxygen vacancies (Figures 3a, 3b and 4b). As described in section 4.1, the enhanced contrast of oxygen atoms adjacent to the line oxygen vacancy is apparently a local distortion of the bridge oxygen rows surrounding the line oxygen vacancy. Considering an enhanced contrast of bridge oxygen rows surrounding a line oxygen vacancy and an unstable structure of line oxygen vacancy by removal of many oxygen atoms, however, it may be possible to consider that the line oxygen vacancy forms the reconstructed structure. Although it is difficult to confirm the displacement of bridge oxygen rows surrounding the line oxygen vacancy as described in section 4.1, we consider that the reconstructed line vacancies may be active sites for water dissociation. In the line oxygen vacancy, structure changes are therefore due to the structures surrounding the line oxygen vacancy, and these changes might yield active water dissociation sites.

We confirmed the reproducibility of the hydroxyl chain structures formed on line oxygen vacancy by other successive NC-AFM measurements under water atmosphere. Figure 4 results revealed that a hydroxyl chain structure was formed on two rows of the line oxygen vacancy and the right side of the bridge oxygen row adjacent to the line vacancy. Other successive NC-AFM measurements also observed that the hydroxyl chain was formed on two rows of the line oxygen vacancy and the left side of the bridge oxygen row adjacent to the line vacancy. In other words, the hydroxyl chain on the line oxygen vacancy linearly appeared in a form of two rows on the line oxygen vacancy and along either side of the bridge oxygen row adjacent to the line vacancy. However irregular adsorption of hydroxyl groups on the three rows of the line oxygen vacancy and the both side of bridge oxygen rows adjacent to the line vacancy was not observed by successive NC-AFM measurements. The water dissociation mechanism at a line oxygen vacancy is not yet clear. Further study is needed to clarify the processes for hydroxyl chain formation on defective TiO_2(110) surfaces that have line oxygen vacancies.

Previously reported HREELS measurements indicated that water dissociation at oxygen vacancy sites has little or no impact on the electronic structure of TiO_2(110) surfaces.[15] This means that dissociative adsorption of water does not oxidize oxygen vacancy sites. Therefore, when hydroxyl chains are formed at a line oxygen vacancy, the hydroxyl chain on the line oxygen vacancy should have higher charge density than the hydroxyl chain on the bridge oxygen rows. If the charge density of the Ti^{3+} ions in the line oxygen vacancy is reflected in the NC-AFM image contrast, then the contrast of the hydroxyl chains on the line oxygen vacancy and the bridge oxygen row should differ. However, in our study, the image contrast of the hydroxyl chains did not differ (Figures 3a, 3b and 4b).

Using UHV−STM, Maksymovych et al.[40] studied adsorption of H_2O on a TiO_2(110)−(1 × 2) surface and observed line vacancies, which were formed by collective removal of oxygen atoms along the [001] direction on the TiO_2(110)−(1 × 2) surface by UV irradiation.[41] When this surface was exposed to water at 300 K, although dissociative adsorption of water preferentially occurred at the cross-links of the TiO_2(110)−(1 × 2) surface at 300 K, water did not adsorb on the line vacancies.[41]

Maksymovych et al.[40] considered that the line vacancies correspond to partially reduced Ti cations, which are weaker Lewis acids than Ti^{4+} cations and might show little or no reactivity toward water molecules. Considering the line vacancy structure on the TiO_2(110)−(1 × 2) surface, the distance between the line vacancy site and the nearest anion site is about 1.3 nm.[40] Therefore, water molecules might not be dissociatively adsorbed on the line vacancy site because water molecules on this vacancy site cannot interact with the nearest anion sites. In summary, reconstructed line oxygen vacancies on the reduced TiO_2(110)−(1 × 1) surface may be suitable sites for water dissociation.

5. Conclusions

In this study, hydroxyl chains consisting of linearly arranged hydroxyl groups were successfully formed on a reduced TiO_2-(110) surface that had line oxygen vacancies. When the density of oxygen vacancies on the TiO_2(110) surface was increased to 2.0×10^{13} cm^{-2}, a line oxygen vacancy appeared. These (1 × 2) reconstruction structures corresponded not to added-row structures but to missing-row structures formed by removal of oxygen atoms on the bridge oxygen row. After the TiO_2(110) surface with line oxygen vacancies was exposed to water at RT, NC-AFM measurements revealed hydroxyl chain structures on the TiO_2(110) surface. These hydroxyl chain structures were formed by the hydroxyl groups being arranged in a form of two rows on the line oxygen vacancy and on a neighboring bridge oxygen row. In-situ NC-AFM measurements of the TiO_2-(110) surface before and after exposure to water revealed that the hydroxyl chain structure was formed at the line oxygen vacancy. In the NC-AFM images, the bridge oxygen rows surrounding the line oxygen vacancies showed brighter contrast than did other bridge oxygen rows. This enhanced brightness of the bridge oxygen rows was attributed to a local reconstruction in the line oxygen vacancies, suggesting that the line oxygen vacancies might change structure into a suitable site for water dissociation. Based on the NC-AFM measurements, line oxygen vacancies are active sites for dissociative adsorption of water on TiO_2(110) surface. In conclusion, the formation of a hydroxyl chain structure suggests that the surface hydroxyl groups on a TiO_2(110) surface can be controlled by preparing oxygen vacancy structures on the surface.

Acknowledgment. We gratefully acknowledge Prof. H. Onishi, Dr. C. L. Pang, Dr. A. Sasahara, and Dr. R. Tero for fruitful discussions.

References and Notes

(1) Kung, H. H. *Transition Metal Oxides: Surface Chemistry and Catalysis*; Elsevier: Netherlands, 1989.

(2) Henrich, V. E.; Cox, P. A. *The Surface Science of Metal Oxides*; Cambridge University Press: Cambridge, 1994.

(3) Diebold, U. *Surf. Sci. Rep.* **2003**, *48*, 53.

(4) Suzuki, S.; Fukui, K.; Onishi, H.; Iwasawa, Y. *Phys. Rev. Lett.* **2000**, *84*, 2156.
(5) Henderson, M. A. *Surf. Sci. Rep.* **2002**, *46*, 1.
(6) Pan, J. M.; Maschhoff, B. L.; Diebold, U.; Madey, T. E. *J. Vac. Sci. Technol. A* **1992**, *10*, 2470.
(7) Kurtz, R. L.; Stockbauer, R.; Madey, T. E.; Roman, E.; Segovia, J. L. D. *Surf. Sci.* **1989**, *218*, 178.
(8) Henderson, M. A. *Surf. Sci.* **1996**, *355*, 151.
(9) Henderson, M. A. *Langmuir* **1996**, *12*, 5093.
(10) Henderson, M. A. *Surf. Sci.* **1998**, *400*, 203.
(11) Henderson, M. A.; Tapia, S. O.; Castro, M. E. *Faraday Discuss.* **1999**, *114*, 313.
(12) Brookes, I. M.; Muryn, C. A.; Thornton, G. *Phys. Rev. Lett.* **2001**, *87*, 266103/1.
(13) Schaub, R.; Thostrup, P.; Lopez, N.; Lægsgaard, E.; Stensgaard, I.; Nørskov, J. K.; Besenbacher, F. *Phys. Rev. Lett.* **2001**, *87*, 266104/1.
(14) Fujino, T.; Katayama, M.; Inudzuka, K.; Okuno, T.; Oura, K.; Hirao, T. *Appl. Phys. Lett.* **2001**, *79*, 2716.
(15) Henderson, M. A.; Epling, W. S.; Peden, C. H. F.; Perkins, C. L. *J. Phys. Chem. B* **2003**, *107*, 534.
(16) White, J. M.; Szanyi, J.; Henderson, M. A. *J. Phys. Chem. B* **2003**, *107*, 9029.
(17) Suzuki, S.; Fukui, K.; Onishi, H.; Sasaki, T.; Iwasawa, Y. *Stud. Surf. Sci. Catal.* **2001**, *132*, 753.
(18) *Noncontact Atomic Force Microscopy*; Morita, S.; Wiesendanger, R.; Meyer, E.; Eds.; Springer: New York, 2002.
(19) Fukui, K.; Onishi, H.; Iwasawa, Y. *Phys. Rev. Lett.* **1997**, *79*, 4202.
(20) Fukui, K.; Iwasawa, Y. *Noncontact Atomic Force Microscopy*; Morita, S., Wiesendanger, R., Meyer, E., Eds.; Springer: New York, 2002; pp 167−181.
(21) Alberecht, T. R.; Grütter, P.; Horne, D.; Rugar, D. *J. Appl. Phys.* **1991**, *69*, 668.
(22) Meyer, E.; Howald, L.; Lüthi, R.; Haefke, H.; Rüetschi, M.; Bonner, T.; Overney, R.; Frommer, J.; Hofer, R.; Güntherodt, H. J. *J. Vac. Sci. Technol. B* **1994**, *12*, 2060.
(23) Howald, L.; Lüthi, R.; Meyer, E.; Güntherodt, H. J. *Phys. Rev. B* **1995**, *51*, 5484.
(24) Fukui, K.; Namai, Y.; Iwasawa, Y. *Appl. Surf. Sci.* **2002**, *188*, 252.
(25) Namai, Y.; Fukui, K.; Iwasawa, Y. *J. Phys. Chem. B* **2003**, *107*, 11666.
(26) Namai, Y.; Fukui, K.; Iwasawa, Y. *Catal. Today* **2003**, *85*, 79.
(27) Onishi, H.; Iwasawa, Y. *Surf. Sci.* **1994**, *313*, L783.
(28) Onishi, H.; Fukui, K.; Iwasawa, Y. *Bull. Chem. Soc. Jpn.* **1995**, *68*, 2447.
(29) Onishi, H.; Iwasawa, Y. *Phys. Rev. Lett.* **1996**, *76*, 791.
(30) Takakusagi, S.; Fukui, K.; Nariyuki, F.; Iwasawa, Y. *Surf. Sci.* **2003**, *523*, L41.
(31) Pang, C. L.; Haycock, S. A.; Raza, H.; Murray, P. W.; Thornton, G.; Gülseren, O.; James, R.; Bullett, D. W. *Phys. Rev. B* **1998**, *58*, 1586.
(32) Bannett, R. A.; Stone, P.; Price, N. J.; Bowker, M. *Phys. Rev. Lett.* **1999**, *82*, 3831.
(33) Bannett, R. A.; Stone, P.; Bowker, M. *Faraday Discuss.* **1999**, *114*, 267.
(34) Fischer, S.; Munz, A. W.; Schierbaum, K. D.; Göpel, W. *Surf. Sci.* **1995**, *337*, 17.
(35) Fischer, S.; Schierbaum, K. D.; Göpel, W. *J. Vac. Sci. Technol. B* **1996**, *14*, 961.
(36) Fischer, S.; Munz, A. W.; Schierbaum, K. D.; Göpel, W. *Vacuum* **1997**, *48*, 601.
(37) Diebold, U. *Appl. Phys. A* **2003**, *76*, 681.
(38) Ng, K. O.; Vanderbilt, D. *Phys. Rev. B* **1997**, *56*, 10544.
(39) Lindan, P. J. D.; Harrison, N. M.; Gillan, M. J.; White, J. A. *Phys. Rev. B* **1997**, *55*, 15919.
(40) Maksymovych, P.; Mezhenny, S.; Yates, J. T., Jr. *Chem. Phys. Lett.* **2003**, *382*, 270.
(41) Mezhenny, S.; Maksymovych, P.; Thompson, T. L.; Diwald, O.; Stahl, D.; Walck, S. D.; Yates, J. T., Jr. *Chem. Phys. Lett.* **2003**, *369*, 152.